Article

Reversible Scavenging of Dioxygen from Air by a Copper Complex

Kurtis M. Carsch,‡ Andrei Iliescu,‡ Ryan D. McGillicuddy, Jarad A. Mason, and Theodore A. Betley*

Read Online

ACCESS | Metrics & More | Article Recommendations | Supporting Information

ABSTRACT: We report that exposing the dipyrrin complex (^{EMind}L)Cu(N$_2$) to air affords rapid, quantitative uptake of O$_2$ in either solution or the solid-state to yield (^{EMind}L)Cu(O$_2$). The air and thermal stability of (^{EMind}L)Cu(O$_2$) is unparalleled in molecular copper-dioxygen coordination chemistry, attributable to the ligand flanking groups which preclude the [Cu(O$_2$)]$^{1+}$ core from degradation. Despite the apparent stability of (^{EMind}L)Cu-(O$_2$), dioxygen binding is reversible over multiple cycles with competitive solvent exchange, thermal cycling, and redox manipulations. Additionally, rapid, catalytic oxidation of 1,2-diphenylhydrazine to azoarene with the generation of hydrogen peroxide is observed, through the intermittency of an observable (^{EMind}L)Cu(H$_2$O$_2$) adduct. The design principles gleaned from this study can provide insight for the formation of new materials capable of reversible scavenging of O$_2$ from air under ambient conditions with low-coordinate Cu^I sorbents.

O$_2$ Manipulation through Solvent, Temperature, and Redox
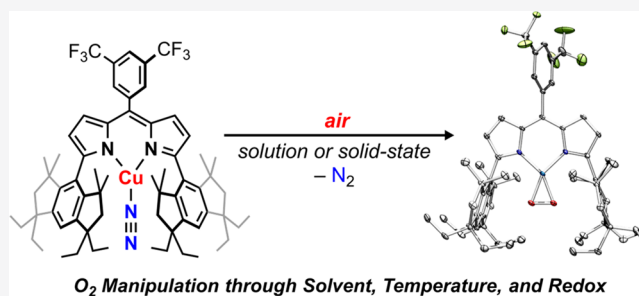
1. INTRODUCTION

The industrial separation of high-purity dioxygen (O$_2$) from air is of paramount importance for chemical synthesis[1,2] with myriad applications in oxy-fuel combustion, medical treatments, and steel manufacturing.[3] The current methodology for O$_2$ purification involves desiccating and filtration of air, followed by fractional distillation at both cryogenic temperatures and elevated pressures to remove undesirable components, primarily dinitrogen (N$_2$). Distillation purification of O$_2$ is currently conducted on scales exceeding 100 Mton annually.[4] The direct separation of O$_2$ from humid, unpurified air without the requisite desiccation, particulate filtration, and intermittent cryogenic distillation would represent an advancement in O$_2$ separations. Various N$_2$-selective cation-exchanged zeolites[5] and O$_2$-selective metal–organic frameworks with coordinately unsaturated metal ions[6−14] have demonstrated promise for O$_2$ separation from binary O$_2$/N$_2$ mixtures under milder conditions; however, the water sensitivity of these activated frameworks and their diminished capacity over multiple cycles at ambient temperatures hinders wide-scale implementation in O$_2$ separation. Fine tuning the O$_2$ binding site at the molecular level may yet enable new strategies to achieve selective O$_2$ separation from air.

Nature employs selective O$_2$ binding in metalloenzymes for O$_2$ transport.[15,16] In particular, the Cu^I sites in hemocyanin[17] reversibly binds O$_2$, inspiring a number of biomimetic Cu-based model complexes.[18−20] In contrast to metalloenzymes, synthetic copper-dioxygen complexes suffer from poor thermal stability and poor control of nuclearity, attributable to the absence of the protein superstructure which modulates substrate access to avoid framework degradation.[21] In general, the binding and activation of O$_2$ by molecular complexes is well-established;[22−26] yet synthetic complexes often suffer from facile O$_2$ displacement without excess O$_2$,[27] low O$_2$ affinity in the solid-state,[28,29] ligand oxidative degradation,[30] or irreversible O$_2$ activation.[31] Thus, an ideal transition metal–ligand combination would preserve low coordination numbers for the bound transition metal, lack activatable functionalities for oxidative robustness, and facilitate O$_2$ binding reversibly.

Recently, we described an isolable, triplet copper-nitrene supported by a dipyrrin scaffold featuring sterically encumbered peralkylated hydridacene EMind[32] substituents (EMind: 1,1,7,7-tetraethyl-1,2,3,5,6,7-hexahydro-3,3,5,5-tetramethyl-*s*-indacene).[33] The Cu resides in a hydrophobic, sterically protected pocket ideal for stabilizing traditionally reactive species. Herein, we report the preparation of an air-stable, side-bound cupric superoxide (^{EMind}L)Cu(O$_2$) which displays remarkable aqueous, thermal, and vacuum stability. Nonetheless, O$_2$ displacement can be promoted using a variety of stimuli. The bound O$_2$ can also be converted to hydrogen peroxide catalytically via arylhydrazine oxidation under ambient air. These observations of using reversible O$_2$ binding to a low-coordinate Cu^I site provides new design insights for the generation of new O$_2$ separation materials.

2. RESULTS AND DISCUSSION

2.1. Cu Oxygenation. During routine manipulations of $(^{EMind}L)Cu(N_2)$ **(1)**,[33] we observed a rapid color change from orange to red upon exposure of **1** to ambient air to yield **2** (Figures 1a and S23). This color change from **1** to **2** was
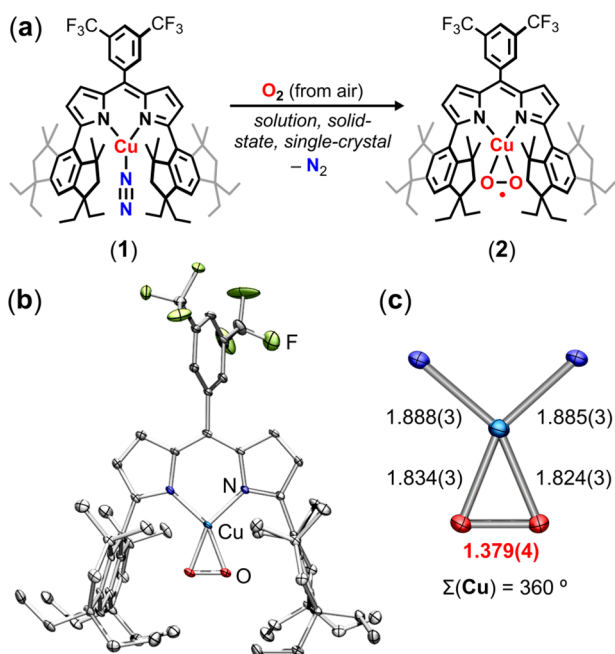

Figure 1. (a) Air exposure of $(^{EMind}L)Cu(N_2)$ **(1)** affords thermally robust $(^{EMind}L)Cu(O_2)$ **(2)** in quantitative yield in either solution or the solid state. (b) Solid state structure of **2** at 100 K depicted at 50% displacement ellipsoid probability. (c) Pertinent bond metrics in the $[Cu(O_2)]^{1+}$ core. Color scheme: Cu (cobalt blue), F (yellow-green), N (blue), and O (red).

distinct from the yellow-orange hue attributed to free ligand $(^{EMind}L)H$, arguing against ligand protonolysis from atmospheric water, which is prevalent in $3d$ transition metal dipyrrin complexes. In hexanes, the color change upon air exposure was accompanied by notable effervescence, consistent with loss of

the coordinated dinitrogen ligand from **1**. Analysis by UV/vis spectroscopy revealed a subtle red-shift in the Soret band ($\lambda_1 = 515$ cm^{-1}, $\varepsilon_1 = 65\,000$ M^{-1} cm^{-1}; $\lambda_2 = 520$ cm^{-1}, $\varepsilon_2 = 59\,000$ M^{-1} cm^{-1}) as well as a substantial blue-shift in a less intense absorbance feature ($\lambda_1 = 400$ cm^{-1}, $\varepsilon_1 = 5200$ M^{-1} cm^{-1}; $\lambda_2 = 360$ cm^{-1}, $\varepsilon_2 = 7000$ M^{-1} cm^{-1}; Figure 2a). Multinuclear ($^1H/^{19}F/^{13}C\{^1H\}$) NMR spectroscopy revealed a single diamagnetic species (Figure 2b, see the Supporting Information for assignments of spectra resonances), accessed in quantitative yield from **1** (Figures S1–S3). A high-resolution mass spectrum of air-exposed **1** was satisfactorily modeled as $[(^{EMind}L)Cu(N_2) + 2O - 2N]^+$, suggesting exchange of the coordinated N_2 for O_2 (Figure S4). Accordingly, single crystal X-ray diffraction at 100 K on crystals produced from a concentrated pentane solution of **1** under air at −10 °C overnight revealed the corresponding side-bound dioxygen-adduct $(^{EMind}L)Cu(O_2)$ **(2)** (Figure 1b, c).

Interestingly, high-quality single crystals of **2** could be prepared through a single-crystal-to-single-crystal transformation by exposure of **1** to air over 1 week, reflecting the minimal changes in lattice parameters between **1** and **2** as well as the low volatility of the encapsulated pentane solvent molecule within the crystalline lattice (Figure S47). Analysis of the solid-state molecular structure reveals a planar geometry about the Cu ion and relatively short Cu−O bond lengths (1.824(3), 1.834(3) Å) (Figure 2c). The O−O bond length (1.379(4) Å) is comparable to that observed in our previously reported $(^{Ar}L)Cu(O_2)$ (1.383(2) Å; ^{Ar}L: 5-mesityl-1,9-(2,4,6-Ph$_3C_6H_2$)-dipyrrin), assigned as a predominant $Cu^{II}(O_2{}^{\bullet-})$ electronic structure based on the observed bonds lengths and multi-configurational calculations.[34] By analogy, we tentatively assign **2** as a cupric superoxide as a more appropriate descriptor than a high-valent cupryl peroxide $Cu^{III}(O_2{}^{2-})$ formulation. The relatively short $N_{dipyrrin}$−Cu bond parameters (1.888(3), 1.885(3) Å) are similarly comparable to an authentic cupric species in the same dipyrrin platform $(^{EMind}L)CuCl$, (1.901(3), 1.894(3) Å).[33] Resonance Raman studies on **2-$^{16}O_2$** and isotopically labeled $(^{EMind}L)Cu(^{18}O_2)$ **(2-$^{18}O_2$)** reveal an isotopically sensitive feature at 1003 cm^{-1} (shifted 50 cm^{-1} to 953 cm^{-1} for **2-$^{18}O_2$** with an expected shift of 57 cm^{-1} to 946 cm^{-1} for an ideal harmonic oscillator; see the Supporting
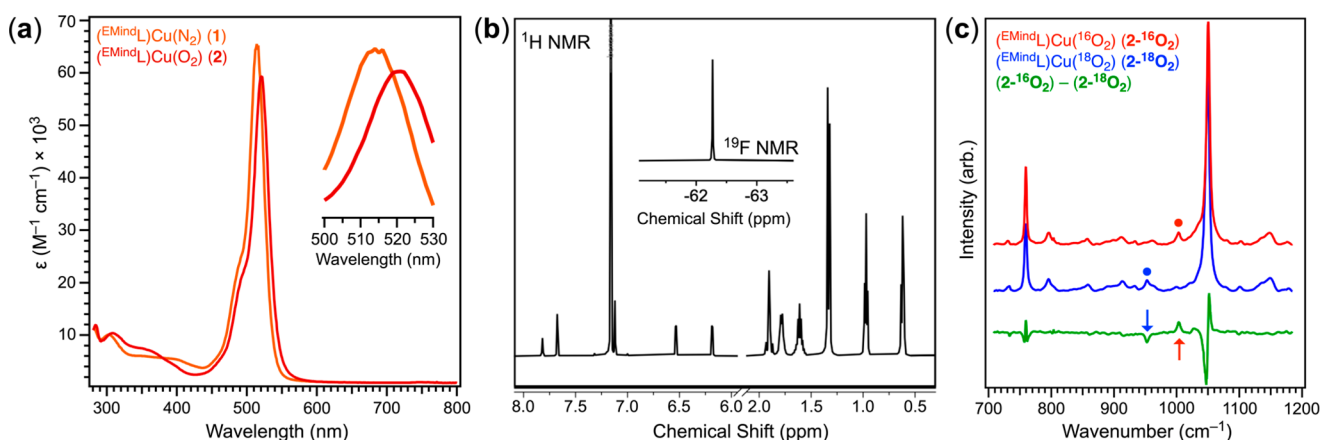

Figure 2. (a) UV/visible spectroscopy depicting shifts in absorbances from $(^{EMind}L)Cu(N_2)$ **(1)** upon air exposure to yield $(^{EMind}L)Cu(O_2)$ **(2)**. Inset depicts the shift in the Soret band. (b) ^{1}H NMR spectrum of **2** in C$_6$D$_6$, displaying diamagnetic resonances. Inset depicts a single resonance by ^{19}F NMR spectroscopy. (c) Resonance Raman measurements on **2-$^{16}O_2$**, displaying an isotopically sensitive resonance at 1003 cm^{-1} (blue) with a shift to 953 cm^{-1} for $^{18}O_2$ labeling (red) most consistent with a superoxide motif. The difference map (green) indicates changes between **2-$^{16}O_2$** and **2-$^{18}O_2$**.
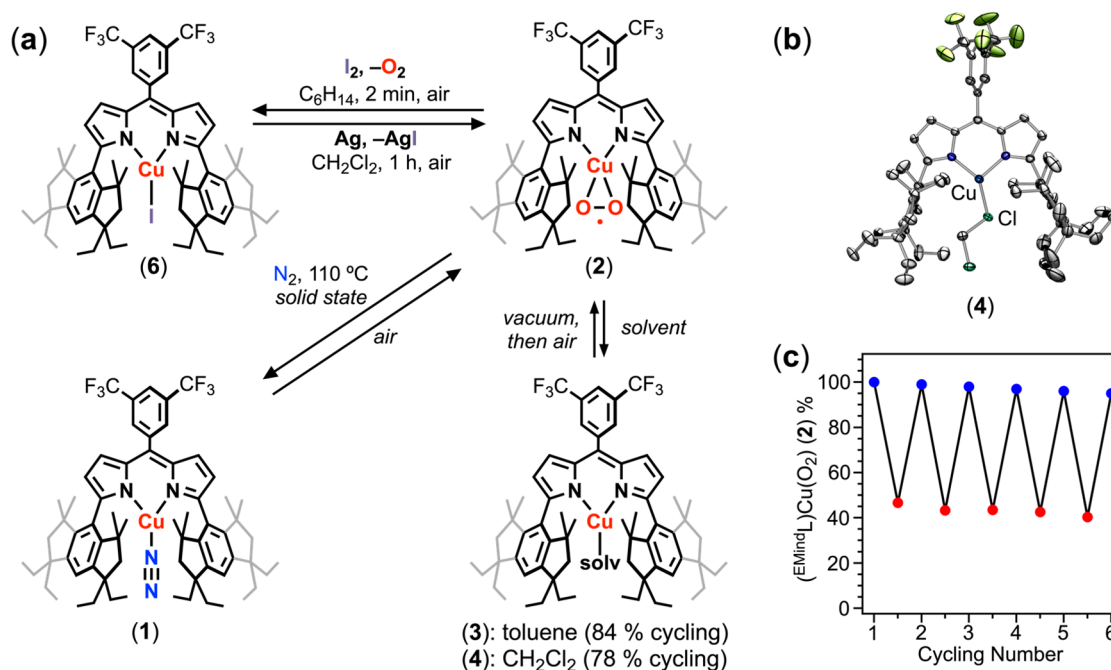
Figure 3. (a) Displacement of O_2 from $(^{EMind}L)Cu(O_2)$ (**2**) through chemical redox, thermolysis under N_2, or solvent ligation. (b) Solid state structure of $(^{EMind}L)Cu(CH_2Cl_2)$ (**4**) at 100 K depicted at 50% displacement ellipsoid probability. Hydrogen atoms of the ligand scaffold are omitted for clarity, excluding those on the hydrazine motif. Color scheme: Cu (cobalt blue), Cl (green), F (yellow-green), N (blue). (c) Thermogravimetric analysis (TGA), illustrating reversible coordination of O_2 under active N_2 flow at 110 °C. Color scheme denotes **2** under N_2 (red) and under O_2 (blue).

Information for synthesis details), in agreement with mononuclear β-diketiminate-supported (968 cm^{-1}) and tris-(pyrazolyl)hydroborate-supported (1043 cm^{-1}) CuO_2 species, both of which display an electronic structure most consistent with a predominant cupric superoxide formulation (Figure 2c).[19,35]

2.2. Stability Assessment. The steric protection afforded by the hydrindacene units engenders both kinetic persistence and thermodynamic stability, preventing protolytic decomposition products and oligomerization. No noticeable decomposition was observed upon aqueous workup of **2** in aliphatic solvents. Thermogravimetric analysis (TGA) measurements on crystalline **2** illustrate no apparent decomposition below 120 °C under active flow of Ar, pure O_2, or air. Allowing crystalline **2** to stand at 100 °C under dynamic vacuum for 36 h afforded no decomposition as evident by multinuclear NMR spectroscopy, conducted by dissolution in C_6D_6 under Ar following thermolysis without intermittent air exposure. Similarly, crystalline samples of **2** left under air for one year show no signs of degradation or substantial changes in crystallinity based on periodically collected single crystal X-ray diffraction data sets. Prolonged thermolysis of a solution of **2** in C_6D_6 (at 10–30 mM concentrations) at 60 °C over multiple days reveals no starting material consumption by ^{1}H/^{19}F NMR spectroscopy. Nonetheless, thermolysis at elevated temperatures under air (80 °C in solution, 150 °C in the solid-state) afforded partial, albeit incomplete, decomposition of **2** to $(^{EMind}L)H$ over a 24 h period (Figure S42), accompanied by deposition of a precipitate.

2.3. Displacement of O_2. Despite the apparent stability of **2**, removal of O_2 could be accomplished through deliberate solvation, redox processes, or thermolysis. Addition of IMes$_2$Pd in C_6D_6 to solid **2** under N_2 afforded $(^{EMind}L)Cu(\eta^2\text{-}C_6H_6)$ and IMes$_2$Pd(O_2), consistent with O_2 transfer (Figure S25).[36]

Whereas dissolution of **2** in C_6D_6 under air failed to elicit O_2 release, dissolution of **2** in neat d_8-toluene (C_7D_8) afforded rapid effervescence with a color change from red to orange-red with the formation of a single diamagnetic species by multinuclear NMR spectroscopy assigned as $(^{EMind}L)Cu(\eta^2\text{-}C_7H_8)$ (**3**) (Figures 3a, S26, and S27). The same spectroscopic features were accessed upon dissolution of crystalline **1** in toluene under N_2, accompanied by the release of N_2. Mixtures of **2** and **3** could be observed from titration of **2** with varying quantities of toluene. Although single crystals of **3** have remained elusive, crystallization of **1** under Ar in the presence of benzene affords $(^{EMind}L)Cu(\eta^2\text{-}C_6H_6)$, featuring an η^2-interaction between the Cu center and rotationally disordered arene (Figure S55).[37] Interestingly, removal of solvent from **3** under vacuum at room temperature afforded **2** (84% yield, ^{1}H/^{19}F NMR, C_6D_6) with partial remaining **3** (16% yield, ^{1}H/^{19}F NMR), producing 0.84 equiv of O_2 per cycle (Figures S28 and S29). These cycling experiments could be performed at least five times with no apparent degradation and with consistent ratios of **2**:**3** upon removal of excess toluene. Similarly, dissolution of **2** in neat dichloromethane rapidly furnished a new diamagnetic species $(^{EMind}L)Cu(CH_2Cl_2)$ (**4**) (**4**, 95%; **2**, 5% remaining) with reformation of **2** (**2**, 83% yield; **4**, 17% remaining) upon evacuation and air exposure, producing 0.78 equiv of O_2 per cycle (Figures 3c and S30–S33). Single crystals of the dichloromethane adduct **4** were isolated under Ar, demonstrating that solvent binding facilitates O_2 displacement (Figure 3b). An extensive screen of additional solvents including cyclic alkenes, ketones, amides, sulfoxides, and sulfur-containing solvents revealed partial or irreversible O_2 displacement with diminished efficacies compared to those of toluene for generating **3** and dichloromethane for generating **4** (Table S1). Strongly coordinating
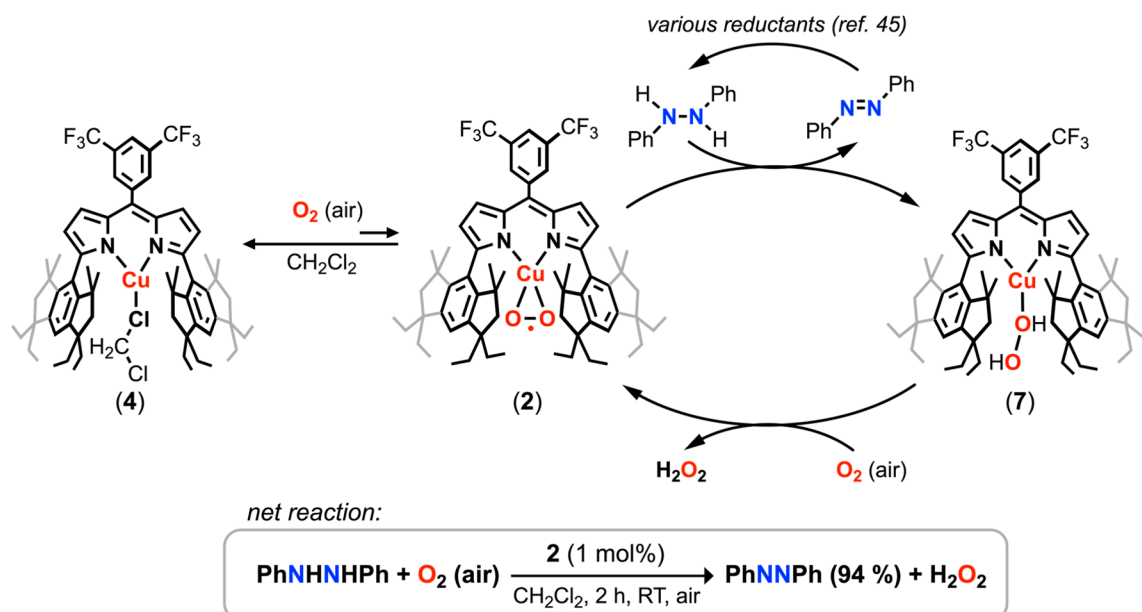
Figure 4. Proposed catalytic cycle for hydrogen peroxide formation through 1,2-diphenylhydrazine oxidation, accompanied by azoarene formation. The off-cycle formation of $(^{EMind}L)Cu(CH_2Cl_2)$ (**4**) is proposed to augment stability of the catalyst toward H_2O_2.

additives such as pyridine and acetonitrile irreversibly displaced O_2 to yield air-stable Cu^I species.

Although d_6-benzene solutions of **2** display indefinite stability in air, dissolution of **2** in C_6D_6 under a N_2 atmosphere afforded detectable quantities (ca. 10%) of $(^{EMind}L)Cu(\eta^2\text{-}C_6D_6)$ through intermittency of **1**, suggesting O_2 displacement could be affected through N_2 binding (Figures S40 and S41). Monitoring the conversion between **2** and **1** by mass changes through TGA, a sample of finely divided microcrystalline **2** (ca. 10 mg, 0.010 mmol) in the solid state at 110 °C under flowing N_2 (10.0 mL/min) for 24 h showed ca. 50−60% conversion to **1**, with rapid conversion back to **2** upon O_2 or air exposure (Figure 3a, c). Indeed, exposure of **1** to a stoichiometric quantity of O_2 in air afforded **2** in quantitative yield upon mixing. Performing TGA cycling measurements between N_2 and O_2 atmospheres revealed partially conversion of **2** to **1** (see the Supporting Information for experimental details) with approximately 95% **2** upon cycling completion by multinuclear NMR studies (Figures S36 and S37). The incomplete conversion of **2** to **1** under N_2 is attributed to kinetic limitations, consequent of poor or incomplete gas penetration in the bulk sample.

The release of coordinated O_2 could be similarly affected through redox mediation. The addition of iodine to **2** induced rapid effervescence from O_2 dissociation, accompanied by a color change from red to dark pink (Figure 3a). Analysis by multinuclear NMR revealed formation of a single paramagnetic species identified as $(^{EMind}L)CuI$ (**6**) by electron paramagnetic resonance for a doublet species and single crystal X-ray diffraction (Figures S17 and S59). A quasi-reversible reduction was observed by cyclic voltammetry ($E_{1/2} = -0.46$ vs Fc/Fc^{1+}) for **6**, attributed to reduction to the corresponding Cu^I species (Figure S19). Accordingly, treatment of **6** with excess metallic silver (3.0 equiv) in dichloromethane under air (1 h) afforded full consumption of **6**, with reformation of a **2/4** mixture in combined quantitative yield upon filtration and workup (Figures S34 and S35). Exposure of this mixture to I_2 rapidly

reafforded **6** in quantitative yield with effervescence from O_2 dissociation, with no diminished capacity over multiple cycles.

Previously reported copper−dioxygen adducts typically exhibit thermal sensitivity and commonly require cryogenic temperature (e.g., −125 °C,[38] −95 °C,[39] −80 °C[30]), excess O_2, and strictly anhydrous reaction conditions to prepare. Additionally, dimeric and trimeric oligomers are observed as a consequence of insufficient steric protection[30] or prearrangement of the Cu^I centers in a multinucleating scaffold.[40] Two notable exceptions of thermally robust copper-dioxygen adducts include $[((^tBu_3tacn)Cu)_2(\mu\text{-}\eta^2{:}\eta^2\text{-}O_2)][OTf]_2$ (tacn: 1,4,7-triazacyclononane)[41] and $(^{Ar}L)Cu(O_2)$.[34] The former complex, prepared by aerobic oxidation of $[(^tBu_3tacn)Cu]$-[OTf], exhibits a gradual decay over prolonged solvation in polar solvents at room temperature (the thermal stability at elevated temperatures was not reported). The latter complex exhibits a reversible, intramolecular η^2-interaction with one of the *ortho*-phenyl groups from the dipyrrin aryl flanking unit, necessitating excess dioxygen (1 atm) and mild cooling (−15 °C) with dilute samples to promote full conversion to the dioxygen adduct and displace the proximal aryl ring. Furthermore, $(^{Ar}L)Cu(O_2)$ reverts to $(^{Ar}L)Cu$ under reduced pressure, reflecting the entropically favored O_2 displacement. Exposure of $(^{Ar}L)Cu$ to ambient air afforded a minor formation of $(^{Ar}L)Cu(O_2)$ (1.0:6.2 by ^1H NMR for $Cu(O_2)$: Cu), accompanied by gradual decomposition over hours to unidentified paramagnetic species and free ligand, attributed to diminished water stability relative to that of **2** (Figure S24).

2.4. Catalytic O_2 Transfer. The reversible binding of O_2 from **2** prompted us to explore chemical transformations in which **2** could act as a molecular O_2 source. We targeted the catalytic synthesis of hydrogen peroxide from O_2, noting the industrial anthraquinone auto-oxidation process suffers from side reactions in the palladium-catalyzed hydrogenation of the 2-alkylanthraquinone species.[42,43] Direct addition of stoichiometric hydrazine to **2** afforded immediate effervescence to yield the air-stable hydrazine adduct $(^{EMind}L)Cu(NH_2NH_2)$ (**5**) without the generation of hydrogen peroxide (Figure S58).

However, the addition of 1,2-diphenylhydrazine in dichloromethane to **2** (1 mol %) under air at ambient conditions afforded the corresponding azoarene (94% yield) after 2 h (Figures 4 and S49−S51). The azoarene product could be selectively extracted with ethanol to remove dipyrrin-containing species and converted back quantitatively into 1,2-diphenylhydrazine through previously reported chemical reduction protocols.[45] Analysis of the reaction mixture by ^{1}H NMR spectroscopy reveals a diagnostic singlet resonance at δ 9.13 ppm attributable to hydrogen peroxide which could be similarly observed in stock solutions of aqueous H_2O_2 in C_6D_6 (Figure S53). Interestingly, repeating the analogous reaction in hexanes afforded 62% azoarene over 2 h with an observation of (^{EMind}L)H and full consumption of **2** by ^{1}H NMR spectroscopy, suggesting the partial equilibrium between **2** and **4** in CH_2Cl_2 may prevent ligand hydrolysis from the acidic hydrogen peroxide. Consistent with this hypothesis, (^{EMind}L)H was rapidly observed upon exposure of **2** to silica in neat hexanes, whereas we observed no free ligand (^{EMind}L)H upon flash column chromatography (silica) in neat dichloromethane of **4**. For comparison, the autoxidation of 1,2-diphenylhydrazine to azoarene and hydrogen peroxide under an O_2 atmosphere in the absence of **2** required ca. 48 h to observe the corresponding azoarene (92% yield). By contrast, trace formation (13% yield) of azoarene was formed under ambient air after 2 h in the absence of **2** due to background autoxidation (Figure S52). Similarly low yields of the diazene product were obtained with free ligand (^{EMind}L)H and related Cu^I species (e.g., CuCl, (^{Ar}L)Cu, (^{tBu}L)$_2$Cu$_2$),[44] suggesting the sequestration and stabilization of Cu within the (^{EMind}L) ligand scaffold is necessary for the reaction.

Whereas treatment of **2** under air with stoichiometric 1,2-diphenylhydrazine afforded a combination of azoarene, H_2O_2, and **2**, repeating the analogous experiment under N_2 or Ar afforded azoarene and a new diamagnetic Cu-containing species. Control experiments of **1** with 1,2-diphenylhydrazine and azoarene afforded no changes in ^{1}H NMR resonances. To rule out H_2O generation and coordination following H_2O_2 disproportionation, addition of H_2O to **1** was assessed, affording a separate, air-sensitive diamagnetic species consistent with an aquo complex. Based on these observations, we assign the Cu-containing species resulting from hydrazine oxidation under inert atmosphere as the air-sensitive peroxide adduct (^{EMind}L)Cu(H_2O_2) (**7**). Accordingly, treatment of **1** with anhydrous hydrogen peroxide in the form of $(Ph_3PO)_2(H_2O_2)$[46] afforded the same multinuclear NMR resonances, corroborating our assignment of the previous product as **7** (Figure S22). We note treatment of **1** with triphenylphosphine oxide elicited no changes by ^{1}H NMR spectroscopy. Although isolable adducts of hydrogen peroxide are known,[47−50] prior reports feature hydrogen bond acceptors in the secondary coordination sphere to overcome the poor σ-donating properties of H_2O_2.[50] Density functional theory computations reveal coordination of H_2O_2 is accompanied by no apparent perturbation in H_2O_2 bond metrics, indicative of minimal activation (Figure S54). By contrast, the highly electrophilic Cu center and hydrindacene flanking units promote coordination and thermal stability of the ligated hydrogen peroxide despite the lack of hydrogen bond acceptors in **7**.

3. CONCLUSION

The foregoing data demonstrates a biomimetic approach to molecular oxygen scavenging using a dipyrrin-supported copper complex. The side-bound, superoxide adduct is remarkably robust and can form from ambient air via electron transfer from Cu^I. Release of O_2 could be achieved through solvent displacement, molecular redox processes, and thermolysis under N_2. Rapid oxidation of arylhydrazines with **2** was observed under ambient conditions, generating the corresponding azoarene and hydrogen peroxide. These results suggest that the use of low-coordinate, electrophilic Cu^I frameworks may provide promising platforms for O_2 purification from air. The low oxophilicity of Cu^I makes it ideal for O_2 capture and release, occurring via facile electron transfer to O_2 to form superoxide or peroxide adducts that may be subsequently displaced. Further evidence for this proposal was recently reported showing that a Cu^I metal−organic framework reversibly changes color upon air exposure[14] with isotherm measurements indicating a strong $Cu−O_2$ heat of adsorption. Detailed spectroscopic and computational studies of **2** as well as related dipyrrin-supported O_2 adducts are underway.

■ ASSOCIATED CONTENT

ⓢ Supporting Information

The Supporting Information is available free of charge at https://pubs.acs.org/doi/10.1021/jacs.1c10254.

> Materials and methods, synthesis details, ^{1}H NMR, ^{13}C NMR, and ^{19}F NMR spectra, EPR spectra, cyclic voltammograms, XRD refinement details, pertinent bond metrics, and solid-state structures of compounds (PDF)

Accession Codes

CCDC 2049906−2049910 contain the supplementary crystallographic data for this paper. These data can be obtained free of charge via www.ccdc.cam.ac.uk/data_request/cif, or by emailing data_request@ccdc.cam.ac.uk, or by contacting The Cambridge Crystallographic Data Centre, 12 Union Road, Cambridge CB2 1EZ, UK; fax: +44 1223 336033.

■ AUTHOR INFORMATION

Corresponding Author

Theodore A. Betley − Department of Chemistry and Chemical Biology, Harvard University, Cambridge, Massachusetts 02138, United States; orcid.org/0000-0001-5946-9629; Email: betley@chemistry.harvard.edu

Authors

Kurtis M. Carsch − Department of Chemistry and Chemical Biology, Harvard University, Cambridge, Massachusetts 02138, United States; orcid.org/0000-0003-4432-7518

Andrei Iliescu − Department of Chemistry and Chemical Biology, Harvard University, Cambridge, Massachusetts 02138, United States

Ryan D. McGillicuddy − Department of Chemistry and Chemical Biology, Harvard University, Cambridge, Massachusetts 02138, United States

Jarad A. Mason − Department of Chemistry and Chemical Biology, Harvard University, Cambridge, Massachusetts 02138, United States; orcid.org/0000-0003-0328-7775

Complete contact information is available at:
https://pubs.acs.org/10.1021/jacs.1c10254

Author Contributions

[‡]K.M.C. and A.I. contributed equally.

Notes

The authors declare no competing financial interest.

■ ACKNOWLEDGMENTS

■ REFERENCES

(1) Smith, A. R.; Klosek, J. A Review of Air Separation Technologies and Their Integration with Energy Conversion Processes. *Fuel Process. Technol.* **2001**, *70*, 115.

(2) Kirschner, M. J.; Alekseev, A.; Dowy, S.; Grahl, M.; Jansson, L.; Keil, P.; Lauermann, G.; Meilinger, M.; Schmehl, W.; Weckler, H. Oxygen. *Ullmann's Encycl. Ind. Chem.* **2017**, 1.

(3) Buhre, B. J.; Elliott, L. K.; Sheng, C.; Gupta, R. P.; Wall, T. F. Oxy-Fuel Combustion Technology for Coal-Fired Power Generation. *Prog. Energy Combust. Sci.* **2005**, *31*, 283.

(4) Greenwood, N. N.; Earnshaw, A. Oxygen. In *Chemistry of the Elements*; Elsevier, 2012.

(5) Nandi, S. P.; Walker, P. L. Separation of Oxygen and Nitrogen Using 5A Zeolite and Carbon Molecular Sieves. *Sep. Sci.* **1976**, *11*, 441.

(6) Jaffe, A.; Ziebel, M. E.; Halat, D. M.; Biggins, N.; Murphy, R. A.; Chakarawet, K.; Reimer, J. A.; Long, J. R. Selective, High-Temperature O$_2$ Adsorption in Chemically Reduced, Redox-Active Iron-Pyrazolate Metal−Organic Frameworks. *J. Am. Chem. Soc.* **2020**, *142*, 14627.

(7) Xiao, D. J.; Gonzalez, M. I.; Darago, L. E.; Vogiatzis, K. D.; Haldoupis, E.; Gagliardi, L.; Long, J. R. Selective, Tunable O$_2$ Binding in Cobalt(II)−Triazolate/Pyrazolate Metal−Organic Frameworks. *J. Am. Chem. Soc.* **2016**, *138*, 7161.

(8) Murray, L. J.; Dinca, M.; Yano, J.; Chavan, S.; Bordiga, S.; Brown, C. M.; Long, J. R. Highly-Selective and Reversible O$_2$ Binding in Cr$_3$(1,3,5-Benzenetricarboxylate)$_2$. *J. Am. Chem. Soc.* **2010**, *132*, 7856.

(9) Bloch, E. D.; Murray, L. J.; Queen, W. L.; Chavan, S.; Maximoff, S. N.; Bigi, J. P.; Krishna, R.; Peterson, V. K.; Grandjean, F.; Long, G. J.; Smit, B.; Bordiga, S.; Brown, C. M.; Long, J. R. Selective Binding of O$_2$ over N$_2$ in a Redox−Active Metal−Organic Framework with Open Iron(II) Coordination Sites. *J. Am. Chem. Soc.* **2011**, *133*, 14814.

(10) Reed, D. A.; Xiao, D. J.; Jiang, H. Z. H.; Chakarawet, K.; Oktawiec, J.; Long, J. R. Biomimetic O$_2$ Adsorption in an Iron Metal−Organic Framework for Air Separation. *Chem. Sci.* **2020**, *11*, 1698.

(11) Bloch, E. D.; Queen, W. L.; Hudson, M. R.; Mason, J. A.; Xiao, D. J.; Murray, L. J.; Flacau, R.; Brown, C. M.; Long, J. R. Hydrogen Storage and Selective, Reversible O$_2$ Adsorption in a Metal−Organic Framework with Open Chromium(II) Sites. *Angew. Chem., Int. Ed.* **2016**, *55*, 8605.

(12) Rosen, A. S.; Mian, M. R.; Islamoglu, T.; Chen, H.; Farha, O. K.; Notestein, J. M.; Snurr, R. Q. Tuning the Redox Activity of Metal−Organic Frameworks for Enhanced, Selective O$_2$ Binding: Design Rules and Ambient Temperature O$_2$ Chemisorption in a Cobalt−Triazolate Framework. *J. Am. Chem. Soc.* **2020**, *142*, 4317.

(13) Oktawiec, J.; Jiang, H. Z.; Vitillo, J. G.; Reed, D. A.; Darago, L. E.; Trump, B. A.; Bernales, V.; Li, H.; Colwell, K. A.; Furukawa, H.; et al. Negative Cooperativity Upon Hydrogen Bond-Stabilized O$_2$ Adsorption in a Redox-Active Metal−Organic Framework. *Nat. Commun.* **2020**, *11*, 3087.

(14) Denysenko, D.; Grzywa, M.; Jelic, J.; Reuter, K.; Volkmer, D. Scorpionate-Type Coordination in MFU-4*l* Metal−Organic Frameworks: Small-Molecule Binding and Activation Upon the Thermally Activated Formation of Open Metal Sites. *Angew. Chem., Int. Ed.* **2014**, *53*, 5832.

(15) Solomon, E. I.; Heppner, D. E.; Johnston, E. M.; Ginsbach, J. W.; Cirera, J.; Qayyum, M.; Kieber-Emmons, M. T.; Kjaergaard, C. H.; Hadt, R. G.; Tian, L. Copper Active Sites in Biology. *Chem. Rev.* **2014**, *114*, 3659.

(16) Sono, M.; Roach, M. P.; Coulter, E. D.; Dawson, J. H. Heme-Containing Oxygenases. *Chem. Rev.* **1996**, *96*, 2841.

(17) Van Holde, K. E.; Miller, K. I. In *Advances in Protein Chemistry*; Elsevier: 1995; Vol. 47, p 1.

(18) Cramer, C. J.; Tolman, W. B. Mononuclear Cu−O$_2$ Complexes: Geometries, Spectroscopic Properties, Electronic Structures, and Reactivity. *Acc. Chem. Res.* **2007**, *40*, 601.

(19) Elwell, C. E.; Gagnon, N. L.; Neisen, B. D.; Dhar, D.; Spaeth, A. D.; Yee, G. M.; Tolman, W. B. Copper−Oxygen Complexes Revisited: Structures, Spectroscopy, and Reactivity. *Chem. Rev.* **2017**, *117*, 2059.

(20) Trammell, R.; Rajabimoghadam, K.; Garcia-Bosch, I. Copper-Promoted Functionalization of Organic Molecules: from Biologically Relevant Cu/O$_2$ Model Systems to Organometallic Transformations. *Chem. Rev.* **2019**, *119*, 2954.

(21) Shook, R. L.; Borovik, A. S. Role of the Secondary Coordination Sphere in Metal-Mediated Dioxygen Activation. *Inorg. Chem.* **2010**, *49*, 3646.

(22) Li, G. Q.; Govind, R. Separation of Oxygen from Air Using Coordination Complexes: A Review. *Ind. Eng. Chem. Res.* **1994**, *33*, 755.

(23) Southon, P. D.; Price, D. J.; Nielsen, P. K.; McKenzie, C. J.; Kepert, C. J. Reversible and Selective O$_2$ Chemisorption in a Porous Metal−Organic Host Material. *J. Am. Chem. Soc.* **2011**, *133*, 10885.

(24) Niederhoffer, E. C.; Timmons, J. H.; Martell, A. E. Thermodynamics of Oxygen Binding in Natural and Synthetic Dioxygen Complexes. *Chem. Rev.* **1984**, *84*, 137.

(25) Sundberg, J.; Cameron, L. J.; Southon, P. D.; Kepert, C. J.; McKenzie, C. J. Oxygen Chemisorption/Desorption in a Reversible Single-Crystal-to-Single-Crystal Transformation. *Chem. Sci.* **2014**, *5*, 4017.

(26) Henrici-Olivé, G.; Olivé, S. Activation of Molecular Oxygen. *Angew. Chem., Int. Ed. Engl.* **1974**, *13*, 29.

(27) Karlin, K. D.; Cruse, R. W.; Gultneh, Y.; Farooq, A.; Hayes, J. C.; Zubieta, J. Dioxygen-Copper Reactivity. Reversible Binding of O$_2$ and Co to a Phenoxo-Bridged Dicopper(I) Complex. *J. Am. Chem. Soc.* **1987**, *109*, 2668.

(28) Vaska, L. Oxygen-Carrying Properties of a Simple Synthetic System. *Science* **1963**, *140*, 809.

(29) Holt, S. L.; DeIasi, R.; Post, B. Crystal Structure of the Oxygen-Inactive Form of Bis(Salicylaldehyde) ethylenediiminecobalt(II). *Inorg. Chem.* **1971**, *10*, 1498.

(30) Cole, A. P.; Root, D. E.; Mukherjee, P.; Solomon, E. I.; Stack, T. D. P. A Trinuclear Intermediate in the Copper-Mediated Reduction of O$_2$: Four Electrons from Three Coppers. *Science* **1996**, *273*, 1848.

(31) Hong, S.; Lee, Y.-M.; Ray, K.; Nam, W. Dioxygen Activation Chemistry by Synthetic Mononuclear Nonheme Iron, Copper and Chromium Complexes. *Coord. Chem. Rev.* **2017**, *334*, 25.

(32) Matsuo, T.; Suzuki, K.; Fukawa, T.; Li, B.; Ito, M.; Shoji, Y.; Otani, T.; Li, L.; Kobayashi, M.; Hachiya, M.; Tahara, Y.; Hashizume, D.; Fukunaga, T.; Fukazawa, A.; Li, Y.; Tsuji, H.; Tamao, K. Synthesis

and Structures of a Series of Bulky "Rind-Br" Based on a Rigid Fused-Ring S-Hydrindacene Skeleton. *Bull. Chem. Soc. Jpn.* **2011**, *84*, 1178.

(33) Carsch, K. M.; DiMucci, I. M.; Iovan, D. A.; Li, A.; Zheng, S.-L.; Titus, C. J.; Lee, S. J.; Irwin, K. D.; Nordlund, D.; Lancaster, K. M.; Betley, T. A. Syntheses of a Copper-Supported Triplet Nitrene Complex Pertinent to Copper-Catalyzed Amination. *Science* **2019**, *365*, 1138.

(34) Iovan, D. A.; Wrobel, A. T.; McClelland, A. A.; Scharf, A. B.; Edouard, G. A.; Betley, T. A. Reactivity of a Stable Copper-Dioxygen Complex. *Chem. Commun.* **2017**, *53*, 10306.

(35) Tomson, N. C.; Williams, K. D.; Dai, X.; Sproules, S.; DeBeer, S.; Warren, T. H.; Wieghardt, K. Re-Evaluating the Cu K Pre-Edge Xas Transition in Complexes with Covalent Metal–Ligand Interactions. *Chem. Sci.* **2015**, *6*, 2474.

(36) Konnick, M. M.; Guzei, I. A.; Stahl, S. S. Characterization of Peroxo and Hydroperoxo Intermediates in the Aerobic Oxidation of N-Heterocyclic-Carbene-Coordinated Palladium(0). *J. Am. Chem. Soc.* **2004**, *126*, 10212.

(37) Although the synthesis of **1** is conducted in benzene, the species isolation from workup and crystallization is identified as (^{EMind}L)Cu(N$_2$) (**1**). Nonetheless, dissolution of **1** in neat benzene yields (^{EMind}L)Cu(η^2-C$_6$H$_6$) (**1-C$_6$H$_6$**), which reverts to **1** upon removal of solvent and exposure to N$_2$, as ascertained by infrared spectroscopy and combustion analysis. For clarity, we refer to **1** either as the crystalline solid or as solutions of (^{EMind}L)Cu(N$_2$) in aliphatic solvents.

(38) Citek, C.; Gary, J. B.; Wasinger, E. C.; Stack, T. D. P. Chemical Plausibility of Cu(III) with Biological Ligation in pMMO. *J. Am. Chem. Soc.* **2015**, *137*, 6991.

(39) Gary, J. B.; Citek, C.; Brown, T. A.; Zare, R. N.; Wasinger, E. C.; Stack, T. D. P. Direct Copper(III) Formation from O$_2$ and Copper(I) with Histamine Ligation. *J. Am. Chem. Soc.* **2016**, *138*, 9986.

(40) Lionetti, D.; Day, M. W.; Agapie, T. Metal-Templated Ligand Architectures for Trinuclear Chemistry: Tricopper Complexes and Their O$_2$ Reactivity. *Chem. Sci.* **2013**, *4*, 785.

(41) Karahalis, G. J.; Thangavel, A.; Chica, B.; Bacsa, J.; Dyer, R. B.; Scarborough, C. C. Synthesis and Catalytic Reactivity of a Dicopper(II) μ-η^2:η^2-Peroxo Species Supported by 1,4,7-Tri-Tert-Butyl-1,4,7-Triazacyclononane. *Inorg. Chem.* **2016**, *55*, 1102.

(42) Campos-Martin, J. M.; Blanco-Brieva, G.; Fierro, J. L. Hydrogen Peroxide Synthesis: An Outlook Beyond the Anthraquinone Process. *Angew. Chem., Int. Ed.* **2006**, *45*, 6962.

(43) Goor, G.; Glenneberg, J.; Jacobi, S. Hydrogen Peroxide. *Ullmann's Encycl. Ind. Chem.* **2000**, 1.

(44) Carsch, K. M.; Lukens, J. T.; DiMucci, I. M.; Iovan, D. A.; Zheng, S.-L.; Lancaster, K. M.; Betley, T. A. Electronic Structures and Reactivity Profiles of Aryl Nitrenoid-Bridged Dicopper Complexes. *J. Am. Chem. Soc.* **2020**, *142*, 2264.

(45) Shi, X. Diazene, 1,2-Diphenyl-. In *Encyclopedia of Reagents for Organic Synthesis*; John Wiley & Sons, Ltd, 2012.

(46) Kadassery, K. J.; Dey, S. K.; Cannella, A. F.; Surendhran, R.; Lacy, D. C. Photochemical Water-Splitting with Organomanganese Complexes. *Inorg. Chem.* **2017**, *56*, 9954.

(47) Wallen, C. M.; Bacsa, J.; Scarborough, C. C. Hydrogen Peroxide Complex of Zinc. *J. Am. Chem. Soc.* **2015**, *137*, 14606.

(48) Wallen, C. M.; Palatinus, L.; Bacsa, J.; Scarborough, C. C. Hydrogen Peroxide Coordination to Cobalt(II) Facilitated by Second-Sphere Hydrogen Bonding. *Angew. Chem., Int. Ed.* **2016**, *55*, 11902.

(49) Wallen, C. M.; Bacsa, J.; Scarborough, C. C. Coordination of Hydrogen Peroxide with Late-Transition-Metal Sulfonamido Complexes. *Inorg. Chem.* **2018**, *57*, 4841.

(50) DiPasquale, A. G.; Mayer, J. M. Hydrogen Peroxide: A Poor Ligand to Gallium Tetraphenylporphyrin. *J. Am. Chem. Soc.* **2008**, *130*, 1812.